Sodium Hydride Clusters in Solid Hydrogen and Neon: Infrared Spectra and Theoretical Calculations

Xuefeng Wang and Lester Andrews*

Department of Chemistry, P.O. Box 400319, University of Virginia, Charlottesville, Virginia 22904-4319

Received: April 10, 2007; In Final Form: May 2, 2007

Laser-ablated sodium atom reactions with H_2 have been investigated in solid molecular hydrogens and neon. The NaH molecule and $(NaH)_{2,3,4}$ clusters were identified by IR spectra with isotopic substitution (HD and D_2) and comparison to frequencies calculated by density functional theory and the MP2 method. The use of *para*-hydrogen enriched samples provides evidence for a $(H_2)_nNaH$ subcomplex surrounded by the solid hydrogen matrix cage. The ionic rhombic $(NaH)_2$ dimer is characterized by strong absorptions at 761.7, 759.1, and 757.0 cm^{-1}, respectively, in solid neon, *para*-hydrogen, and normal hydrogen matrices. The cyclic sodium hydride trimer and tetramer clusters are also observed. Although the spontaneous reaction of two Li and H_2 to form $(LiH)_2$ occurs on annealing in solid H_2, the formation of $(NaH)_2$ requires near uv photoexcitation.

Introduction

The vapor in equilibrium with alkali halide salts at high temperature contains mostly alkali halide monomer and some dimer and higher clusters.[1] The diatomic molecules are highly ionic with large electric dipole moments, and the dimers have double bridge rhombic structures.[2] Common stable sodium chloride is a case in point. The NaCl molecule has an equilibrium bond length of 2.361 Å and a dipole moment of 9.0 D, and the $(NaCl)_2$ molecule has a 2.584 Å Na−Cl dimension, a 101.4° Cl−Na−Cl angle, and the lower vibrational frequencies appropriate for the cyclic structure.[3−7] Theoretical calculations are in agreement with this model.[8]

In contrast, sodium hydride is different, owing in large part to lower thermodynamic stability for the hydride anion compared to chloride anion. As a result the vapor in equilibrium with solid sodium hydride contains mostly hydrogen, sodium, and a small amount of NaH molecules but sufficient for observation of microwave and infrared absorption spectra.[9−11] Sodium hydride is, however, chemically unstable at the temperature required for vaporization of the solid. The high-temperature reaction of sodium and hydrogen has produced sufficient NaH for electronic absorption and fluorescence spectroscopic investigations.[9,12] Accordingly, it will be very difficult to observe $(NaH)_2$ in the gas phase. The lighter lithium hydride molecule is more stable, and the dipole moment has been measured as 5.88 D,[13] and the infrared spectrum recorded,[14] but the $(LiH)_2$ dimer has not yet been observed in the gas phase.

Over the last several years, we have prepared metal hydrides through reaction of the metal atoms with solid hydrogen and have observed infrared spectra of many new metal hydrides trapped in solid hydrogen.[15−17] In this manner, unfavorable thermodynamics can be overcome. In the case of lithium, we have observed the first infrared spectrum of $(LiH)_2$ following the reaction of excited Li_2 in solid hydrogen.[18] Here we apply this method to sodium and form $(NaH)_2$ in solid neon and hydrogen for the observation of its infrared spectrum. Density functional theory frequency calculations confirm this assignment.

* Corresponding author. E-mail: lsa@virginia.edu.

Experimental and Computational Methods

The technique for reacting laser-ablated metal atoms with condensing hydrogen has been described in previous papers and one review article.[15−18] Here the special problem is that sodium metal is soft and care must be taken to apply the necessary laser energy and focus to ablate the proper amount of sodium to facilitate small molecule chemistry. The Nd:YAG laser fundamental [1064 nm, 10 Hz repetition rate, 10 ns pulse width, about 1 mJ/pulse] was focused onto a sodium metal target (fresh cut 10 × 10 × 5 mm piece, reagent grade) mounted on a rod and rotated at 1 rpm, and the ablation plume was bright yellow for the sodium resonance emission. Infrared spectra were recorded at 0.5 cm^{-1} resolution and 0.1 cm^{-1} accuracy on a Nicolet 750 using a Hg−Cd−Te range B detector. Matrix samples were annealed and irradiated by a medium-pressure mercury arc lamp (Osram Sylvania, 175 W) with globe removed. Supporting electronic structure calculations were performed using the Gaussian 03 program system, the B3LYP density functional, and the 6-311++G(3df,3pd) basis.[19]

Results and Discussion

Infrared spectra will be presented for sodium reaction products with hydrogen, and isotopic frequencies for new sodium hydride cluster species will be assigned and substantiated through comparison with vibrational frequencies calculated by density functional theory. Absorptions were observed for hydrogen species that are common to laser-ablated metal experiments with solid hydrogen, but no sodium oxide impurities were found in the spectra.[17,20,21]

Infrared Spectra. Infrared spectra for laser-ablated sodium co-deposited with normal hydrogen are illustrated in Figure 1. A sharp band was observed at 1108.5 cm^{-1} [labeled NaH] in the initial spectrum of this deep green matrix sample. Annealing to 6.0 and to 6.5 K had no effect on the spectrum, but irradiation at >320 nm produced a strong 757.0 cm^{-1} band and associated weaker 775.6 cm^{-1} and strong 442.4 cm^{-1} absorptions [labeled $(NaH)_2$], a weaker 958.9 cm^{-1} band [labeled $(NaH)_3$], and a very weak 1053 cm^{-1} absorption [labeled $(NaH)_4$]. Subsequent

10.1021/jp0727852 CCC: $37.00
Published on Web 06/28/2007

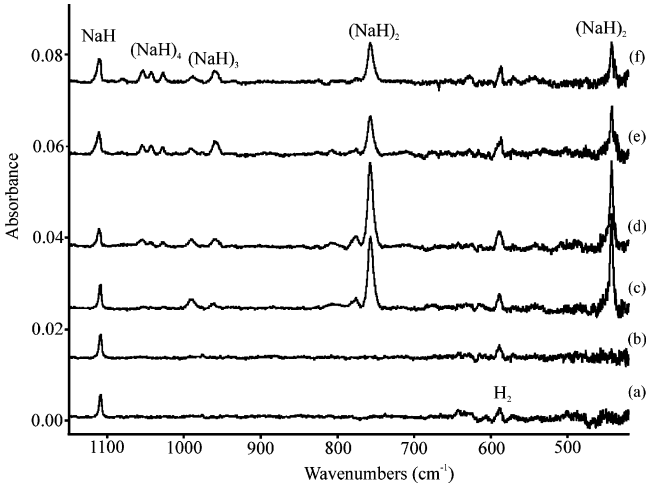

Figure 1. Infrared spectra for sodium atom reaction products with hydrogen: (a) after co-deposition of laser-ablated sodium atoms and hydrogen gas for 30 min at 4 K; (b) after annealing to 6.5 K; (c) after >320 nm irradiaiton; (d) after 240−380 nm irradiation; (e) after >220 nm irradiation; (f) after annealing to 7.0 K.

240−380 nm irradiation increased the $(NaH)_2$ absorptions by 20%, doubled the $(NaH)_3$ band, and markedly increased the 1053.6, 1042.2, and 1027.8 cm^{-1} bands labeled $(NaH)_4$. Full arc (>220 nm) irradiation halved the $(NaH)_2$ bands, and increased the other absorptions. A final annealing to 7 K slightly decreased the $(NaH)_2$ and $(NaH)_3$ absorptions and increased the $(NaH)_4$ bands. The new product absorptions are collected in Table 1.

Analogous results were found using normal deuterium as shown in Figure 2. Sample deposition produced a sharp 805.7 cm^{-1} band and a very weak 555 cm^{-1} absorption. The strong band at 554.8 cm^{-1} and satellite at 567.7 cm^{-1} appeared on ultraviolet irradiation as do weaker broad bands at 698.6, 722.2, and 765.0 cm^{-1}. Annealing increased the latter band at the expense of the others.

Complementary investigations were done with the quantum solids *para*-hydrogen and *ortho*-deuterium,[22,23] and the spectra are compared in Figure 3. The sharp initial product absorptions are at 1121.5 and 810.2 cm^{-1} (labeled NaH and NaD). The major UV irradiation product absorptions are much sharper in these samples at 779.9 and 759.2 cm^{-1} (3.0 cm^{-1} full width at half-maximum) and at 568.5 and 555.7 cm^{-1} (1.5 cm^{-1} bandwidth).

The experiment with Na and pure HD was particularly impressive (Figure 4). The two initial sharp bands were observed at 1118.5 and 813.3 cm^{-1}. Visible irradiation at >470 nm failed to produce product absorptions. Now four sharp new product absorptions were observed at 874.4, 713.6, 605.6, and 510.4 cm^{-1} following ultraviolet irradiation. These bands were produced by >320 nm irradiation, increased with 240−380 nm light, and decreased upon full arc, >220 nm, irradiation.

Neon matrix investigations of the Na and H_2 reaction were fruitful (Figure 5). No NaH was trapped on the initial deposition process, but >320 nm irradiation produced a new 761.7 cm^{-1} band and a weak 966.2 cm^{-1} absorption. Further 240−380 nm irradiation slightly decreased the former and increased the latter and produced a weak new 1049.7 cm^{-1} band. Annealing to 8 K decreased the first two bands and increased the latter band, and final annealing to 9 K decreased the 761.7 cm^{-1} band and increased the 966.2 cm^{-1} absorption. The reaction with D_2 shifted the major bands to 703.0 and 558.6 cm^{-1}. Again, symmetry lowering with the HD reagent gave four product absorptions (labeled NaHNaD).

Calculations. The anticipated major product of the sodium and dihydrogen reaction is $(NaH)_2$, and accordingly calculations were performed following analogous work on $(LiH)_2$.[18] The NaH diatomic molecule was first computed as a calibration because the frequency and bond length are known. Our B3LYP harmonic frequency and distance are 1167.9 cm^{-1} and 1.877 Å, which may be compared to the 1132.8 cm^{-1} infrared absorption and 1.8874 Å bond length observed for the gaseous molecule.[3,11] Although a number of electronic structure and potential energy curve computations have been done for NaH, we are aware of only a few calculations for NaH clusters.[24,25] The analogous stable D_{2h} structure calculated for $(NaH)_2$ is illustrated in Figure 6, and the harmonic frequencies are listed in Table 2. The earlier computations gave slightly longer bond lengths.[25] Calculations were also performed for the cyclic trimer and tetramer structures, as these are expected to be minor products in this system. The natural charge on the metal centers decreases slightly with cluster size, as given in the caption to Figure 6.

NaH. The initial product absorption in normal solid hydrogen at 1108.5 cm^{-1} is below the gas phase NaH fundamental[11] of 1132.8 cm^{-1}, a red shift of 2.1%. By comparison, LiH is red-shifted 4.3% in solid hydrogen.[18] The scale factor for our harmonic B3LYP frequency calculations and our matrix observation is 1108.5/1167.9 = 0.949 for comparison with other sodium hydride species below. However, NaH trapped in the less interacting quantum solids 99.9% *para*-hydrogen and 97.9% HD (molecules in $J = 0$ rotational states)[22] are shifted less to 1121.8 and 1118.5 cm^{-1}, respectively. The harmonic NaH/NaD frequency ratio is 1.3849, and the NaH/NaD ratios for our three pairs of observations are 1.3842, 1.3753, and 1.3758 in the order of decreasing NaH frequencies and increasing interaction with the matrix host. These NaH/NaD ratios reveal an increase in anharmonicity for NaH in the more disorded normal molecular hydrogens than in the more ordered quantum solids. These ratios are between those for lithium and heavier metals and are appropriate for the stretching vibration of hydrogen with a medium weight metal.[14−18]

Following our work on LiH,[18] we suggest that the NaH molecule is trapped in solid hydrogen as a chemical complex $(H_2)_nNaH$, but the binding of hydrogen to the metal center is weaker here. The total binding energies for $n = 1$, 2, and 3 are 3.0, 5.7, and 8.4 kcal/mol, respectively, at the MP2 level of theory, which appears to overestimate the binding energy. The additional solvation effect of replacing *p*-H_2 in the matrix cage with more strongly interacting *o*-H_2 has been investigated for other molecules,[26] and this effect is manifest in our spectra.

We performed additional experiments with laser-ablated sodium and different concentrations of *p*-H_2 in the sample, and the spectra are compared in Figure 7. The sharp 1121.8 cm^{-1} band for the most pure 99.9% *p*-H_2 experiment is followed by a broader 1121.3 cm^{-1} absorption for 95% *para*-hydrogen. The next sample with 85% para enrichment gave a broader band with 1120, middle 1115, and 1109 cm^{-1} component absorptions. Interestingly, annealing this sample to 6.0, to 6.5 and to 7.0 K shifted the peaks and the intensity to lower wavenumbers (Figure 7d−f), and the last spectrum shows peaks at 1115 and 1111 cm^{-1}. Finally, the normal hydrogen product may be compared at 1108.5 cm^{-1}.

Several conclusions can be reached from the spectra in Figure 7, which change as the *para*-hydrogen concentration is decreased when and annealing allows ortho spin state molecules to replace para spin state molecules in the coordination sphere. Recent work has shown that *o*-H_2 molecules ($J = 1$) with a residual quadrupole moment after averaging over the $J = 1$

TABLE 1: Infrared Absorptions (cm^{-1}) Observed for Sodium Hydride and Its Clusters in Different Matrix Samples

neon/H_2	neon/D_2	99% *p*-H_2	normal-H_2	98% *o*-D_2	normal-D_2	HD	assign
		1121.5	1108.5			1118.5	NaH
				810.2	805.7	813.3	NaD
		1057.1	1053.6				$(NaH)_4$ site
1049.7		1049.4	1042.2		765.0		$(NaH)_4$
		1038.6	1027.8				$(NaH)_4$ site
		994.4	989.4		722.2		$(NaH)_3$ site
966.2	703.0	962.8	958.9		698.6		$(NaH)_3$
779 sh		779.3	775.6	568.5	567.7	874.4, 713.6	$(NaH)_2$
761.7	558.6[a]	759.1	757.0	555.7	554.8	605.6, 510.4	$(NaH)_2$
445.0			442.4				$(NaH)_2$

[a] Neon/HD gave 878.3, 714.2, 608.4, and 513.2 cm^{-1} bands for NaHNaD.

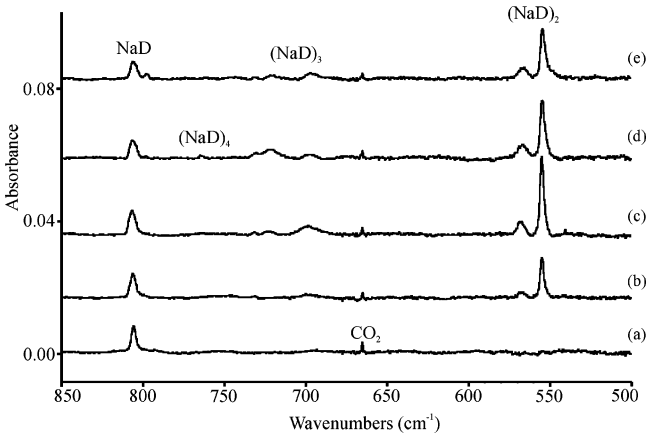

Figure 2. Infrared spectras for sodium atom reaction products with deuterium: (a) after co-deposition of laser-ablated sodium atoms and D_2 for 30 min at 4 K; (b) after >380 nm irradiation; (c) after >290 nm irradiation; (d) after annealing to 9 K; (e) after annealing to 10 K.

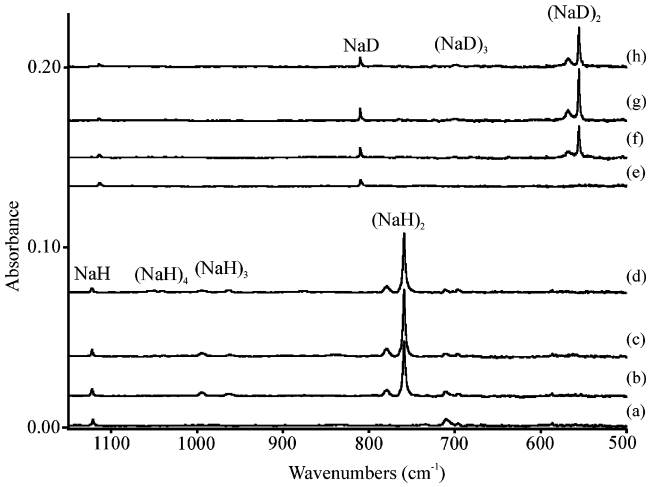

Figure 3. Infrared spectra of sodium atom and *para*-hydrogen or *ortho*-deuterium reaction products: (a) after co-deposition of laser-ablated sodium atoms and 99% *para*-hydrogen for 25 min at 4 K; (b) after >380 nm irradiation; (c) after >290 nm irradiation; (d) after annealing to 7 K; (e) after co-deposition of laser-ablated sodium atoms and 98% *ortho*-deuterium for 25 min at 4 K; (f) after >380 nm irradiation; (g) after >290 nm irradiation; (h) after annealing to 9 K.

rotational wavefunction interact more strongly with guest molecules bearing a dipole moment than *p*-H_2 molecules ($J = 0$) with the quadrupole moment averaging to zero.[26] In effect, the ortho molecules are preferentially attracted to the solute molecule due to stronger intermolecular forces. A recent investigation employed CH_3F (dipole moment 1.86 D) as the guest molecule and found an 8.4 cm^{-1} shift for the gas phase 1048.6 cm^{-1} fundamental in *p*-H_2. We expect NaH with a calculated dipole moment of 6.01 D to attract hydrogen

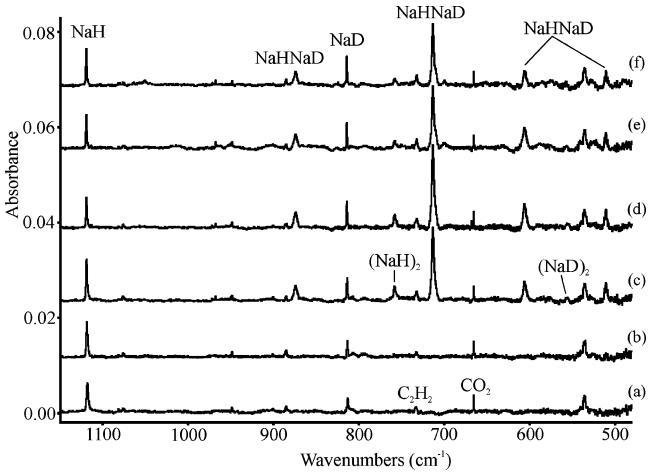

Figure 4. Infrared spectra for Na atom reaction products with mixed H and D reagent: (a) after co-deposition of laser-ablated Na atoms and HD for 30 min at 4 K; (b) after >470 nm irradiation; (c) after >320 nm irradiation; (d) after 240−380 nm irradiation; (e) after >220 nm irradiation; (f) after annealing to 8 K. The weak band at 535.0 cm^{-1} is common to solid HD experiments.

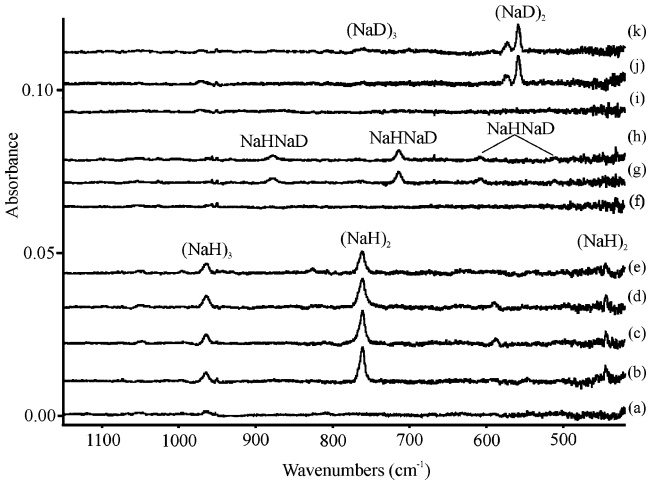

Figure 5. Infrared spectra in for sodium atom reaction products with hydrogen isotopes at 5% in excess neon: (a) after co-deposition of laser-ablated sodium atoms and H_2 for 60 min at 4 K; (b) after >320 nm irradiation; (c) after >240−380 nm irradiation; (d) after annealing to 8 K; (e) after annealing to 9 K; (f) after co-deposition of sodium atoms and HD; (g) after >320 nm irradiation; (h) after 240−380 nm irradiation; (i) after co-deposition of sodium atoms and D_2; (j) after >320 nm irradiation; (k) after 240−380 nm irradiation.

molecules more strongly, and with a large dipole derivative (0.31 ± 0.05 D)[11] to produce a larger gas phase to *para*-hydrogen shift (11.0 cm^{-1} observed). The additional shift from para to normal hydrogen (13.3 cm^{-1}) is due to the replacement of para molecules in the subcomplex and the solvent cage by

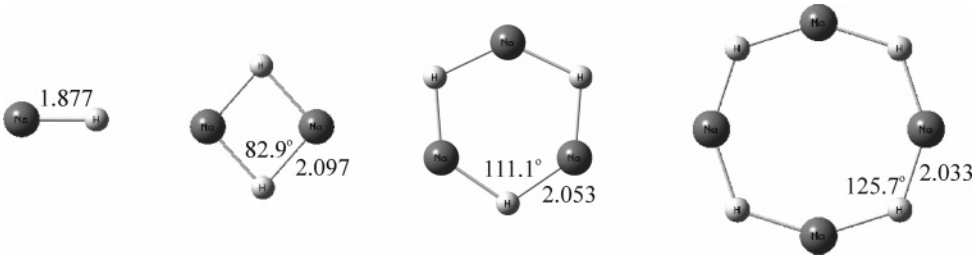

Figure 6. Structures calculated for the NaH, $(NaH)_2$, $(NaH)_3$, and $(NaH)_4$ molecules using the B3LYP/6-311++G(3df,3pd) method. Bond lengths in Å and bond angles in degrees. Natural charges calculated for the metal centers are +0.74, +0.85, +0.83, and +0.84, respectively, in this cluster series.

TABLE 2: Observed and Calculated Frequencies (cm^{-1}) for $(NaH)_2$ Isotopic Molecules (^1A_g in D_{2h} Symmetry)

	$(NaH)_2$			$(NaD)_2$		(NaHNaD)	
mode	obs[a]	cal anh[b]	cal harm[c]	obs	cal harm	obs	cal harm
a_g		949.7	980.9 (0)		696.7 (0)	874.4	924.6 (352)
b_{2u}	775.6	805.1	845.5 (992)	567.7	610.5 (517)	713.6	753.7 (609)
b_{1u}	757.0	762.1	811.3 (905)	554.8	585.8 (472)	605.6	642.5 (403)
b_{3g}		607.5	657.1 (0)		476.9 (0)	510.4	512.0 (80)
b_{3u}	442.4	423.8	455.1 (726)		328.6 (378)		397.3 (552)
a_g		223.8	230.8 (0)		229.8 (0)		230.3 (0)

[a] Observed frequencies from solid H_2 and D_2. [b] Calculated anharmonic frequencies at the B3LYP/6-311++G(3df,3pd) level of theory. [c] Calculated harmonic frequencies with infrared intensities in km/mol.

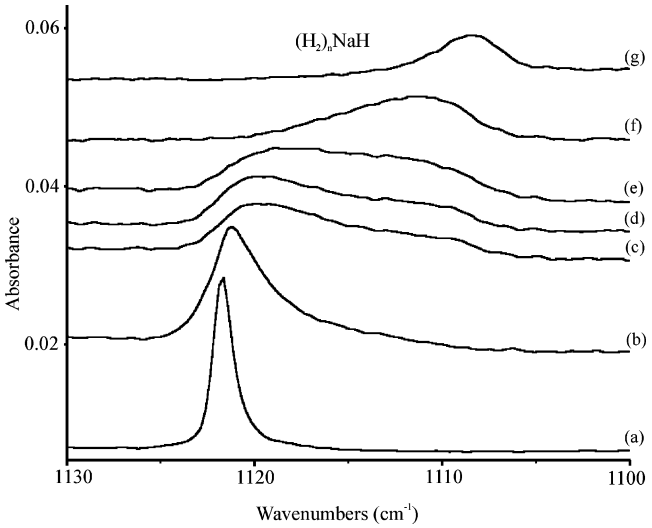

Figure 7. Infrared spectra of laser-ablated sodium atom and *para*-hydrogen−*ortho*-hydrogen mixtures: (a) 99.9% para; (b) 95% para; (c) 85% para; (d) after annealing to 6 K; (e) after annealing to 6.5 K; (f) after annealing to 7.0 K; (g) normal hydrogen.

more strongly interacting ortho molecules, and this is larger than the corresponding 5.7 cm^{-1} shift found for methyl fluoride.[26] The larger hydrogen matrix shift for LiH with a slightly smaller dipole moment (5.88 D) and derivative (0.239 D in the $1 \leftarrow 0$ transition)[13,14] as compared to NaH suggest an overall weaker solvent interaction with the larger NaH molecule.

The band profile in Figure 7 argues strongly for a chemical subcomplex surrounded by a matrix cage of additional hydrogen molecules. A continuous spectrum without subpeaks is expected and observed for CH_3F as *para*-hydrogen cage molecules are replaced by *ortho*-hydrogen.[26] Although we cannot identify the number of dihydrogen molecules in the subcomplex, it is probable that two are involved as found for $(H_2)_2LiH$.[18] Our spectra are believed to arise from three bisdihydrogen complexes that differ by the nuclear spin states of the two dihydrogen ligands, namely $(p\text{-H})_2NaH$, $(p\text{-H})(o\text{-H})NaH$, and $(o\text{-H})_2NaH$, and the more strongly interacting ortho ligand provides additional red shift in the Na−H vibrational chromophore with an additional small dependence on the para/ortho concentration in the surrounding matrix cage.

$(NaH)_2$. The first two photochemical product absorptions at 757.0 and 775.6 cm^{-1} in solid hydrogen shift to 554.8 and 567.7 cm^{-1} in solid deuterium. The H/D frequency ratios, 1.3645 and 1.3662, for this new product show more anharmonicity than the NaH diatomic molecule stretching mode. The strong IR active antisymmetric (b_{1u} motion of H along Na−Na axis and b_{2u} motion of H away from Na−Na axis) stretching modes for $(NaH)_2$ are computed at 811.3 and 845.5 cm^{-1}, respectively, and the (observed frequency)/(harmonic calculated frequency) ratios, 0.933 and 0.917 (the so-called "scale factor"), are almost the same as found for $(LiH)_2$.[18] The scale factors for the $(NaD)_2$ frequencies, 0.947 and 0.930 are, of course, slightly larger as the heavier isotope is less anharmonic, and anharmonicity is not included in the harmonic frequency calculation used for the scale factor. The confirming evidence for this identification is provided by the match of calculated and observed frequencies for NaHNaD (see Figure 4), where symmetry lowering makes all four bond stretching modes IR active. In decreasing frequency order, these are perpendicular and parallel motions of H and then D, respectively, with respect to the Na−Na axis. The observed and calculated harmonic frequencies are compared in Table 2, and the scale factors for the bands observed in HD are 0.946, 0.947, 0.943, and 0.997, which provides excellent correlation between experiment and computation. The constancy of the first three scale factors is as striking as is the difference with the latter, for which we have no explanation as these all involve different amplitudes for the H and D atoms in these in-plane interionic bond stretching vibrational modes. These scale factors are slightly lower than typical scale factors for the B3LYP functional[27] presumably because the ionic NaH bond is more difficult to describe theoretically than the more common covalent bonds.

As also found for the analogous $(LiH)_2$ molecule,[18] the calculated and observed infrared intensities agree only qualitatively. The two antisymmetric Na−H stretching modes are computed to be of comparable intensity, but the b_{2u} mode absorption is weaker and broader (about 1:6 relative integrated intensity). Either the calculation is in error for this highly ionic

TABLE 3: Observed and Calculated Frequencies (cm^{-1}) for Na_3H_3 ($^1A_1'$ in D_{3h} Symmetry)

	Na_3H_3		Na_3D_3	
mode	obs[a]	calc[b]	obs	calc
e″	958.9	1028.3 (675 × 2)	698.6	734.8 (376 × 2)
a_2'		934.3 (0)		677.1 (0)
a_1'		806.7 (0)		571.2 (0)
e′		713.2 (773 × 2)		521.1 (361 × 2)
a_2''		445.2 (1008)		321.5 (525)
e″		243.4 (0 × 2)		182.7 (0)[c]
a_1'		182.8 (0)		178.0 (0 × 2)[c]
e′		113.7 (39 × 2)		111.3 (39 × 2)

[a] Observed frequencies from solid normal H_2 or D_2. [b] Calculated harmonic frequencies at the B3LYP/6-311++G(3df,3pd) level of theory with infrared intensities in km/mol. [c] Mode symmetry switched from H to D.

TABLE 4: Observed and Calculated Frequencies (cm^{-1}) for Na_4H_4 (^1A_g in D_{4h} Symmetry)

	Na_4H_4		Na_4D_4	
mode	obs[a]	calc[b]	obs[a]	calc[b]
b_{1g}		1154.3 (0)		818.7 (0)
e_u	1042.2	1129.7 (1011 × 2)	765	809.2 (551 × 2)
a_{2g}		1059.6 (0)		767.1 (0)
a_{1g}		703.3 (0)		497.5 (0)
e_u		629.7 (943 × 2)		458.4 (0)[c]
b_{2g}		604.4 (0)		458.0 (437 × 2)[c]
a_{2u}[d]		435.8 (1341)		314.7 (700)

[a] Observed frequencies from solid H_2 or D_2. [b] Calculated at the B3LYP/6-311++G(3df,3pd) level of theory. [c] Modes switched from H to D. [d] Another ten lower frequency modes are not listed.

molecule or H_2 matrix interactions with the differently charged Na^+ and H^- alter the relative mode intensity. One can envision that the b_{2u} motion away from the Na−Na axis might be damped by the matrix cage more than the b_{1u} motion along the Na−Na axis.

The absorption bands are a couple of wavenumbers higher in the *para*-hydrogen or *ortho*-deuterium solids and a couple of wavenumbers higher still in solid neon, which are less interacting media than the normal solid molecular hydrogens. Similar behavior was found for LiH.[18] The important NaHNaD absoptions are also observed 1−4 cm^{-1} higher in solid neon than in pure solid HD.

The strong sharp 442.4 cm^{-1} band in solid hydrogen is just below the 455.1 cm^{-1} calculated value for the out-of-plane bending mode of the hydrogen atoms. This band is observed in solid neon at 455.0 cm^{-1} but not in *para*-hydrogen.

$(NaH)_3$. The next product absorption to appear on irradiation shows more stability on annealing, which suggests a higher cluster. The band at 958.9 cm^{-1} in solid hydrogen shifts to 698.6 cm^{-1} in solid deuterium (H/D ratio 1.3726). The neon matrix counterpart at 966.2 cm^{-1} is even more favored on annealing (Figure 5) and the D_2 counterpart at 703.0 cm^{-1} defines a similar 1.3744 ratio. The highest active mode for $(NaH)_3$ is computed at 1028.3 cm^{-1} (Table 3), and if we apply the above 0.933 scale factor from $(NaH)_2$, the frequency is predicted at 959 cm^{-1}, which is in excellent agreement with the observed bands. Our calculation also predicts another strong e′ mode near 700 cm^{-1}, but this band is not observed above our background. The analogous lower $(LiH)_3$ band was much weaker than predicted by calculation. The calculations apparently do not predict infrared intensities as accurately for ionic molecules like $(NaH)_2$ and $(NaH)_3$ as for covalent molecules. This may arise because of the predominantly electrostatic bonding in the alkali hydride clusters.[25b] On the other hand, the matrix may interact differently with the positive and negative charge centers and significantly alter the IR intensities of these two normal modes.

$(NaH)_4$. The last product absorptions to grow on higher energy irradiation and to increase at the expense of the above bands on annealing appear as a trio at 1053.6, 1042.2, and 1027.8 cm^{-1} and a single deuterium counterpart is observed weakly at 765 cm^{-1} (H/D ratio 1.362). The neon matrix counterpart of the former is 1049.7 cm^{-1}. Similar behavior was found for the analogous lithium species.[18] The next higher cluster, the cyclic tetramer has a still higher frequency IR active mode calculated at 1129.7 cm^{-1} (Table 4), and the same 0.933 scale factor predicts this mode at 1054 cm^{-1}, which is in excellent agreement with the observed bands. At the SCF level the cubic tetramer has comparable energy,[25a] but the longer internuclear distances argue for lower frequencies, as we found for Li_4H_4.[18] The earlier SCF calculations also find a decrease in Na−H distance with increasing cluster size, as we show in Figure 6, and these workers point out that chain-like structures will give way to the more solid-like structures with sufficiently large cluster size. Our matrix isolation experiments do not allow large enough clusters to form and fold into the crystal structure.

Reaction Mechanisms. The reaction mechanism is revealed by the use of the HD mixed isotopic reagent. The product bands on deposition of laser-ablated sodium with HD are due to NaH and NaD, and the major photochemical product is clearly NaHNaD with very small amounts of $(NaH)_2$ and $(NaD)_2$ molecules detected as well (Figure 4). [The latter pure isotopic molecule absorptions at 758.3 and 556.5 cm^{-1} in solid HD are 1−2 cm^{-1} higher than their values in the normal hydrogen and normal deuterium solids.] This means that most of the $(NaH)_2$ product in these experiments is formed by reaction with the H_2 reagent, and that a small amount comes from the dimerization reaction (1), which is an exothermic process. However, note that the dimerization of LiH is more exothermic (ΔE = −45 kcal/mol).[18] In contrast to the $(LiH)_2$ case, annealing failed to produce the less stable $(NaH)_2$ dimer, as the dimerization energy for two Na atoms (−17 kcal/mol) is not enough to activate reaction (2). The threshold for the photochemical formation of $(NaH)_2$ in solid hydrogen is between 470 and 380 nm and it appears to be near 420 nm based on the appearance of $(NaH)_2$ at this wavelength in our best *para*-hydrogen experiment. This is appropriate for the Franck−Condon absorption of Na_2 from the ground $^1\Sigma_g^+$ state to the $^1\Pi$ state.[28] Such an absorption band has been assigned at 470 nm in solid argon, but the assignment of electronic bands to sodium cluster species in solid matrix samples is not an exact science.[29,30] Nevertheless, the gas phase work predicts a Na_2 absorption in this region, and the hydrogen matrix will not shift this absorption significantly. Thus, the Na_2 absorption in solid hydrogen will be in the region of our threshold for the photochemical production of $(NaH)_2$. Even though reaction (3) is essentially thermoneutral for the ground state reagents, the electronic excitation of Na_2 in the violet spectral region is more than enough to drive the reaction (3). As is also the case for LiH species, higher cluster formation on annealing is an exothermic process, but more so for LiH clusters.[18] It appears that NaH monomers can add to the smaller cyclic clusters to form larger cyclic clusters, but at

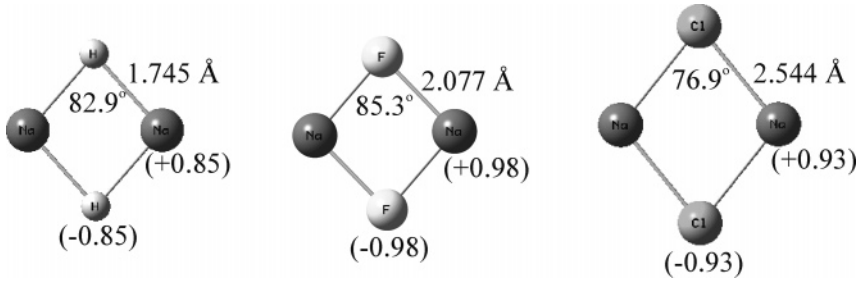

Figure 8. Structures calculated for the rhombic $(NaH)_2$, $(NaF)_2$, and $(NaCl)_2$ molecules using the B3LYP/6-311++G(3df,3pd) method. Bond lengths in Å and bond angles in degrees. Natural sodium atomic charges are +0.85, +0.98, and +0.93.

sufficiently large cluster size, more compacted solid-like structures will ultimately form.

$$NaH + NaH \rightarrow (NaH)_2 \qquad [\Delta E = -33 \text{ kcal/mol}]^{31} \quad (1)$$

$$Na + Na + H_2 \rightarrow Na_2^* + H_2 \nrightarrow (NaH)_2 \qquad [\Delta E = +0.3 \text{ kcal/mol}] \quad (2)$$

$$Na_2 + H_2 + \text{blue vis irrad} \rightarrow Na_2^* + H_2 \rightarrow (NaH)_2 \qquad [\Delta E = +0.3 \text{ kcal/mol}] \quad (3)$$

$$NaH + (NaH)_2 \rightarrow (NaH)_3 \qquad [\Delta E = -37 \text{ kcal/mol}] \quad (4)$$

$$NaH + (NaH)_3 \rightarrow (NaH)_4 \qquad [\Delta E = -32 \text{ kcal/mol}] \quad (5)$$

Bonding. The rhombic $(NaH)_2$ molecule is highly ionic, like the isostructural $(LiH)_2$ molecule, first observed in solid hydrogen where unfavorable thermodynamics can be overcome,[18,32] and like the more stable and thus better known sodium halide dimers[8] (Figure 8). The bridge bond stretching modes for $(NaH)_2$ at 775.6 and 757.0 cm^{-1} are 70 and 68% of the NaH monomer frequency at 1108.5 cm^{-1} in solid hydrogen. In like fashion, our $(LiH)_2$ stretching fundamentals are 75 and 69% of the LiH frequency in solid hydrogen.[18] The isostructural $(NaCl)_2$ molecule exhibits strong bridge bond stretching modes at 272 and 226 cm^{-1}, which are 81 and 67% of the 335.8 cm^{-1} NaCl fundamental in solid argon.[6,7] These lower frequencies relative to the isolated monomer are typical of bridge bond stretching modes involving an M−H−M coordinate.[13−15]

The more stable sodium halide dimers are formed in more highly exothermic reactions than $(NaH)_2$. The dipole moments of NaF and NaCl are larger (B3LYP calculated values 8.0 and 8.7 D, respectively) than the calculated value for NaH (6.0 D), and the latter has yet to be measured experimentally.

$$NaF + NaF \rightarrow (NaF)_2 \qquad [\Delta E = -57 \text{ kcal/mol}] \quad (6)$$

$$NaCl + NaCl \rightarrow (NaCl)_2 \qquad [\Delta E = -46 \text{ kcal/mol}] \quad (7)$$

It is interesting to consider the bonding molecular orbitals of $(NaH)_2$ (Figure 9) and to see that in reation 3 electron density is removed from the region between the two sodium atoms and donated to the more electronegative hydrogen atoms to form the two bridge bonds. In this manner the Na−Na distance in the Na_2 molecule (B3LYP calculated 3.039 Å) with two weak valence bonding electrons is in fact longer than the nonbonded Na−Na distance (2.777 Å) held in position by the electrostatic forces operating within the four ion Na_2H_2 system.[25b] Note that the $(NaH)_2$ molecule is slightly more ionic than $(LiH)_2$, based on calculated natural charges[33] on the metal centers, +0.85 and +0.84, respectively, and this can be seen from close comparison of the highest two calculated molecular orbitals at the same iso density level.[18]

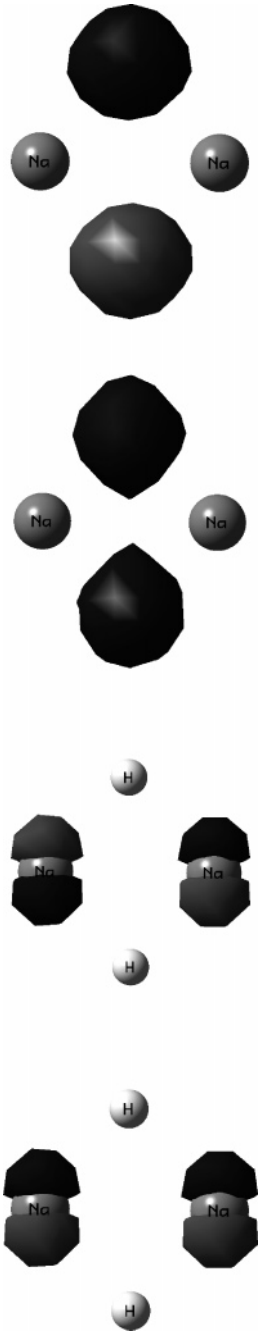

Figure 9. Highest four occupied molecular orbitals calculated for $(NaH)_2$ using the B3LYP method. The iso value of electron density is 0.07 e/au^3. The highest energy orbital is at the top and the orbital energy decreases going down.

Conclusions

Laser-ablated sodium atoms condensed with hydrogen gas at 4 K give the NaH reaction product, which is trapped as a $(H_2)_nNaH$ complex in the solid hydrogen lattice. The effect of H_2 nuclear spin state in the primary complex and the secondary matrix cage ranges from the sharp 1121.8 cm^{-1} absorption in 99.9% *p*-H_2 to the broader 1108.5 cm^{-1} band in normal hydrogen.

Near-ultraviolet irradiation activates the Na_2* reaction with the solid hydrogen matrix and yields strong absorptions for $(NaH)_2$ and also a weak band for $(NaH)_3$. Ultraviolet irradiation and further annealing favor the higher cluster $(NaH)_4$. The sodium hydride dimer is definitively identified though the observation of four absorptions for the lower symmetry NaH-NaD molecule, which are in very good correlation with frequencies calculated by density functional theory. We report here the first observation of sodium hydride clusters, which are shown by computation to be highly ionic.

Acknowledgment. We gratefully acknowledge support for this work from NSF Grant CHE 03-52487.

References and Notes

(1) Klemperer, W.; Norris, W. G. *J. Chem. Phys.* **1961**, *34*, 1071.
(2) Davidovits, P., McFadden, D. L., Eds. *Alkali Halide Vapors*; Academic Press: New York, 1979.
(3) Huber, K. P.; Herzberg, G. *Constants of Diatomic Molecules*; Van Nostrand-Reinhold: New York, 1979.
(4) *Handbook of Chemistry and Physics*, 87th ed.; Chemical Rubber Publishing Co.: Boca Raton, FL, 2006.
(5) Mawhorter, R.; Fink, M.; Hartley, J. G. *J. Chem. Phys.* **1985**, *83*, 4418.
(6) Ismail, Z. K.; Hauge, R. H.; Margrave, J. L. *J. Mol. Spectrosc.* **1975**, *54*, 402.
(7) Howard, W. F., Jr.; Andrews, L. *Inorg. Chem.* **1975**, *14*, 767.
(8) Dickey, R. P.; Maurice, D.; Cave, R. J. Mawhorter, R. *J. Chem. Phys.* **1993**, *98*, 2182.
(9) Sastry, K. V. L. N.; Herbst, E.; DeLucia, D. F. *J. Chem. Phys.* **1981**, *75*, 4753 and references therein.
(10) Leopold, K. R.; Zink, L. R.; Evenson, K. M.; Jennings, D. A. *J. Mol. Spectrosc.* **1987**, *122*, 150.
(11) Maki, A. G.; Olson, W. B. *J. Chem. Phys.* **1989**, *90*, 6887.
(12) Dagdigian, P. J. *J. Chem. Phys.* **1976**, *64*, 2609.
(13) (a) James, T. C.; Norris, W. G.; Klemperer, W. *J. Chem. Phys.* **1960**, *32*, 728. (b) Wharton, L.; Gold, L. P.; Klemperer, W. *J. Chem. Phys.* **1960**, *33*, 1255.
(14) Yamada, C.; Hirota, E. *J. Chem Phys.* **1988**, *88*, 6702.
(15) (a) Wang, X.; Andrews, L. *Inorg. Chem.* **2005**, *44*, 610 (Be + H_2) (b) Wang, X.; Andrews, L. *J. Phys. Chem. A* **2004**, *108*, 11511 (Mg + H_2). (c) Andrews, L.; Wang, X. *Science* **2003**, *299*, 2049. (d) Wang, X.; Andrews, L. Tam, S.; DeRose, M. E.; Fajardo, M. *J. Am. Chem. Soc.* **2003**, *125*, 9218 (Al + H_2).
(16) (a) Wang, X.; Andrews, L. *J. Am. Chem. Soc.* **2002**, *124*, 5636 (WH_6). (b) Wang, X.; Andrews, L. *J. Phys. Chem. A* **2003**, *107*, 570 (Cr + H_2). (c) Wang, X.; Andrews, L. *J. Phys. Chem. A* **2005**, *109*, 9021 (Mo + H_2).
(17) Andrews, L. *Chem. Soc. Rev.* **2004**, *33*, 123 and references therein.
(18) (a) Wang, X.; Andrews, L. *Angew. Chem., Int. Ed.* **2007**, *46*, 2602. (b) Wang, X.; Andrews, L. *J. Phys. Chem. A* **2007**, *111*, 6008.
(19) Kudin, K. N.; Burant, J. C.; Millam, J. M.; Iyengar, S.S.; Tomasi, J.; Barone, V.; Mennucci, B.; Cossi, M.; Scalmani, G.; Rega, N.; Petersson, G. A.; Nakatsuji, H.; Hada, M.; Ehara, M.; Toyota, K.; Fukuda, R.; Hasegawa, J.; Ishida, M.; Nakajima, T.; Honda, Y.; Kitao, O.; Nakai, H.; Klene, M.; Li, X.; Knox, J.E.; Hratchian, H. P.; Cross, J. B.; Adamo, C.; Jaramillo, J.; Gomperts, R.; Stratmann, R. E.; Yazyev, O.; Austin, A. J.; Cammi, R.; Pomelli, C.; Ochterski, J. W.; Ayala, P. Y.; Morokuma, K.; Voth, G. A.; Salvador, P.; Dannenberg, J. J.; Zakrzewski, V. G.; Dapprich, S.; Daniels, A. D.; Strain, M. C.; Farkas, O.; Malick, D. K.; Rabuck, A. D.; Raghavachari, K.; Foresman, J. B.; Ortiz, J. V.; Cui, Q.; Baboul, A. G.; Clifford, S.; Cioslowski, J.; Stefanov, B. B.; Liu, G.; Liashenko, A.; Piskorz, P.; Komaromi, I.; Martin, R. L.; Fox, D. J.; Keith, T.; Al-Laham, M. A.; Peng, C. Y.; Nanayakkara, A.; Challacombe, M.; Gill, P. M. W.; Johnson, B.; Chen, W.; Wong, M. W.; Gonzalez, C.; Pople, J. A. *Gaussian 03*, revision B.04; Gaussian, Inc.: Pittsburgh, PA, 2003, and references therein.
(20) Andrews, L.; Wang, X. *J. Phys. Chem. A* **2004**, *108*, 3879 (H/H_2).
(21) Andrews, L. *J. Phys. Chem.* **1969**, *73*, 3922.
(22) Silvera, I. F. *Rev. Mod. Phys.* **1980**, *52*, 393.
(23) Andrews, L.; Wang, X. *Rev. Sci. Instrum.* **2004**, *75*, 3039.
(24) (a) http://srdata.nist.gov/cccbdb. (b) Yang, C.-L.; Zhang, X.; Han, K. L. *J. Mol. Structure (THEOCHEM)* **2004**, *676*, 209 and references therein.
(25) (a) Rupp, M.; Ahlrichs, R. *Theoret. Chim. Acta* **1977**, *46*, 117. (b) Kremer, T.; Harder, S.; Junge, M.; Schleyer, P. v. R. *Organometallics* **1996**, *15*, 585. (c) Baskin, C. P.; Bender, C. F.; Kollman, P. A. *J. Am. Chem. Soc.* **1973**, *95*, 5868.
(26) (a) Yoshioka, K.; Anderson, D. T. *J. Chem. Phys.* **2003**, *119*, 4731 and references therein. (b) Yoshioka, K.; Anderson, D. T. *J. Mol. Struct.* **2006**, *786*, 123.
(27) (a) Scott, A. P.; Radom, L. *J. Phys. Chem.* **1996**, *100*, 16502. (b) Andersson, M. P.; Uvdal, P. L. *J. Phys. Chem. A* **2005**, *109*, 2937.
(28) Demtroder, W.; McClintock, M.; Zare, R. N. *J. Chem. Phys.* **1969**, *51*, 4595.
(29) Welker, T.; Martin. T. P *J. Chem. Phys.* **1979**, *70*, 5683.
(30) Tam, S.; Fajardo, M. E. *J. Chem. Phys.* **1993**, *99*, 854.
(31) B3LYP energy calculations using zero point corrections.
(32) Dagdigian, P. J. *J. Chem. Phys.* **1976**, *64*, 2609.
(33) Reed, A. E.; Curtiss, L. A.; Weinhold, F. *Chem. Rev.* **1988**, *88*, 899.